CEA TECHNOLOGIE
DIVISION DE METALLURGIE ET D'ETUDES DES COMBUSTIBLES NUCLEAIRES

D.TECH/SECS/LMA 82 - 167
D.TECH/SECS/LECI 82 - 650
FR8307615

THE CARBURIZATION OF ABSORBING ELEMENT CLADDING IN FAST BREEDER REACTORS

R. CYTERMANN+, J.P. SAGOT++, J. ROUAULT+++

Specialist meeting on absorbing pins and materials
San-Francisco, CA, USA 11-15 Apr 1983
CEA-CONF--6658

+ Département de Technologie, S.E.C.S.

++ Département de Technologie, S.R.M.A.

+++ Département d'Etude des Combustibles à Base de Plutonium, S.L.H.A.

CENTRE D'ETUDES NUCLEAIRES DE SACLAY
91191 GIF-sur-YVETTE CEDEX

THE CARBURIZATION OF ABSORBING ELEMENT CLADDING IN FAST BREEDER REACTORS

R. Cytermann, J.P. Sagot and J. Rouault

ABSTRACT

The phenomenon of carburization in the cladding of absorbing elements in fast breeder reactors was studied by the techniques of X-ray microanalysis and micro-hardness. A comparison of the results obtained for different types of pins showed that the intensity and depth of the carburization were closely dependent on the amount of free carbon present in the boron carbide.

An assessment was made of the effects of the stresses produced within the cladding.

Mechanical properties were in general little affected ; however, in the case of the most severely carburized pin a distinct loss of ductility was observed.

RESUME

Le phénomène de carburation des gaines d'éléments absorbants de la filière à neutrons rapides a été mis en évidence à l'aide des techniques de microanalyse X et de microdureté. La comparaison des résultats obtenus pour différents types d'aiguilles a montré que l'intensité et la profondeur de carburation sont étroitement liées à la quantité de carbone libre existant dans le carbure de bore.

Les effets des contraintes engendrées dans la gaine ont été évalués et notamment les niveaux importants existant en début d'irradiation.

Les propriétés mécaniques sont de manière générale peu affectées ; cependant dans le cas de l'aiguille la plus carburée, on observe une perte sensible de ductilité.

INTRODUCTION

Carburization of the austenitic steel cladding of the absorbing pins in fast breeder reactors may be a factor restricting operational efficiency. Such carburization is liable to have an adverse effect on the mechanical properties of the cladding and, above all, to cause serious embrittlement [1] (fig. 1).

The origin of the phenomenon appears to be connected with the presence of free carbon in the boron carbide and with the carbon liberated as the boron is consumed. This carbon diffuses within the sodium, where its activity rapidly comes to exceed its initial level in the cladding steel. If the temperature is sufficiently high, ($T > 450°C$), all the thermodynamic requirements will have been met for a carbon flux to develop between the sodium and the steel.

Since the solubility of carbon in austenite is extremely low [2] (13 p.p.m. at 600°C and 50 p.p.m. at 700°C for a steel containing 18% of chromium and 8% of nickel), the carbon diffusion within the steel will be accompanied by a phenomenon of precipitation of type $M_{23}C_6$ carbides, the kinetic appearance of which will be essentially dependent on temperature.

In the first part of this paper the effective carburization of the absorbing pin cladding will be examined, as revealed by the X-ray microanalysis and micro-hardness techniques. The consequences of the phenomenon will then be explored, particularly the effects of the stresses produced in the cladding as a result of the carbide precipitation. Lastly, measurement of a series of mechanical properties on sample sections of pins irradiated in PHENIX will enable an assessment to be made of the actual practical effect of the carburization.

1 - CHARACTERISTICS OF THE PINS EXAMINED

1.1 - Characteristics of the cladding and of the boron carbide

The absorbing pin cladding examined are of type 316 steel with an initial carbon content of 745 p.p.m. The following chart shows the main characteristics of this material.

Type of pin / Characteristic	Type 1 pin	Type 2 pins
Grain-size ASTM	8	6 to 8
$E_{0.2\%}$ in daN/mm²	61	65
Tensile strength R max in daN/mm²	80	77
Elongation Total A%	24	26
C %	0,0745	0,07
Si %	0,45	0,65
Mn %	1,9	1,53
Cr %	16,9	17,34
Ni %	13,5	13,6
Mo %	2,17	2,17
Inner dia. in mm.	∿ 26	∿ 26
Outer dia. in mm.	∿ 28	∿ 28
Gap separating from absorber in mm.	∿ 1	∿ 1

CHART I. CHARACTERISTICS OF THE CLADDING

It should further be noted that two types of boron carbide had been used for the control rod pins examined, namely :

a. A standard PHENIX type (Type 1).

b. A modified version of the standard type (Type 2), produced by a manufacturing process so adapted as to decrease the quantity of free carbon.

1.2 - Irradiation data

The chart below gives all the main irradiation data for the different types of pins examined :

Type of pin / Parameter	Type 1 pin 1A and 1B	Type 2 pins	
		2A	2B and 2C
No. of days operating	368	304	428
Equivalent no. at max. capacity (J.E.P.P.)	292	229	357
dpaF max.	53	41	57
Average depth in mm	293	294	290
Maximum dose in $n\alpha/cm^3$	93.10^{20}	77.10^{20}	120.10^{20}
Consumption in B^{10} in %	18	15,5	24,3
Maximum temperature inside cladding in °C	500 ± 20	500 ± 20	500 ± 20

CHART II. IRRADIATION DATA

2 - DEMONSTRATION OF THE CARBURIZATION PHENOMENON

Following the discovery of the carburization problem, as demonstrated by global chemical analysis, a method was evolved for measuring the local carbon concentration in irradiated austenitic steels with the aid of X-ray microanalysis techniques [3, 4, 5, 6]. The fine measurements effected at a serie of individual points, with the aid of which a profile may be determined for the radial distribution of the carbon through the cladding, are of particular interest compared with the methods previously used for studying carburization, i.e. global chemical analysis and qualitative measurement by the micro-hardness method. The first of these two methods affords no more than average values of the carbon concentration in the cladding and does not enable an evaluation to be made of the depth of the carburized area. Measurement by micro-hardness, though it enables the depth of the carbon penetration to be approximately determined, is unfortunately influenced by other parameters, so that, as it can be seen from Fig. 2 [4], there exists no correct and univocal relation between micro-hardness and carbon content.

The carburization phenomenon was therefore essentially studied with the aid of carbon concentration profiles obtained with a shielded electron micro-probe. Results showed distinct variation according to the type of boron carbide (standard or modified) used for the pins.

2.1 - Type 1 pin (1A and 1B)

A a general rule the measuring was done every ten micro-meters, starting from the inner face of the cladding.

Figs. 3 and 4 show the progression of the carbon content in a radial direction in claddings1A and 1B. The rectangles drawn round each point chosen correspond to the possible margins of error with regard to the position of the probe spot and in the counting.

The first of the measured points, located only 10 micro-meters from the face of the cladding, is the subject of greater uncertainty owing to the extremity effects.

The following points emerge from a study of the concentration profiles :

a. The surface concentrations (after extrapolation) are respectively 1 and 1.5%.

b. The depths of carburization are in the region of 120 and 160 µm these values agree most satisfactorily with those derived from the profiles obtained by the micro-hardness method (Fig.5).

For the purpose of estimating the variations in carburization on different portions of the circumference, a number of different measurements were also effected 20µm from the inner face for pin 1B. The results are given in Chart III.

Ref. N°7	Carbon concentration %
1	0,52 ± 0,08
2	0,41 ± 0,07
3	0,32 ± 0,07
4	0,43 ± 0,07
5	0,28 ± 0,10
6	0,47 ± 0,17
7	0,55 ± 0,07
8	0,66 ± 0,08
9	0,74 ± 0,07
10	0,80 ± 0,07

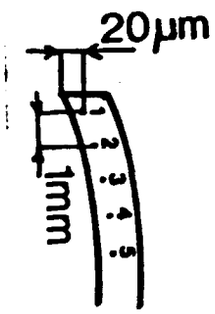

CHART III - MEASUREMENTS EFFECTED 20 µm FROM THE INNER FACE OF PIN 1B

Taken as a whole the carbon contents thus recorded are relatively similar (average 0.52% ; standard deviation 0.17%), although the minimum and maximum values are respectively 0.28 and 0.80%

2.2 - Type 2 pins

a) Pin 2A

The analyses made on different sections revealed uniform carburization ; a typical case is illustrated in Fig.6.

Chart IV shows the main characteristics of the distribution profiles.

Section	Surface of concentration of Cs %	Depth of carburization in µm
X1 radius 1	0,35	50
X1 radius 2	0,75	60
X2	0,50	120
X3	0,60	70
X4	0,70	60

CHART IV. INTENSITY OF CARBURIZATION OBSERVED IN THE CLADDING OF PIN 2A

These various results taken jointly, and the measurements effected 20 µm from the inside face of the cladding, reflect the roughly uniform nature of the carburization in the portion of cladding examined (sample sections taken in the bottom of the pin : 0 to 20 mm).

b) Pins 2B and 2C

As a general rule the claddings of these pins show little carburization.

Chart V gives all the measurements obtained at 20 µm from the inner face of the cladding on the three sections of pin 2B examined and demonstrates the very low degree of carburization.

Ref. N°	Carbon concentration %		
	X1	X2	X3
1	0,28 ± 0,04	0,21 ± 0,04	0,08 ± 0,03
2	0,17 ± 0,04	0,24 ± 0,04	0,10 ± 0,04
3	0,14 ± 0,04	0,16 ± 0,05	0,13 ± 0,04
4	0,06 ± 0,04	0,19 ± 0,05	0,09 ± 0,03
5	0,14 ± 0,04	0,18 ± 0,05	0,11 ± 0,03
6	0,17 ± 0,04	0,15 ± 0,06	0,12 ± 0,03
7	0,18 ± 0,04	0,15 ± 0,04	0,12 ± 0,03
8	0,23 ± 0,04	0,20 ± 0,05	0,12 ± 0,03
9	0,18 ± 0,04	0,15 ± 0,06	0,14 ± 0,04
10	0,15 ± 0,04	0,18 ± 0,04	0,12 ± 0,03
11	0,25 ± 0,04	0,18 ± 0,04	
12		0,24 ± 0,04	
13		0,40 ± 0,08	
14		0,22 ± 0,06	
15		0,27 ± 0,06	

CHART V. CONCENTRATION 20µm FROM THE INNER FACE OF THE CLADDING OF PIN 2B

In the case of sections X2 and X3 it was further possible to determine two carbon distribution profiles in a radial direction through the cladding (Fig.7). The chart below gives the main characteristics of these.

Section	Surface Concentration Cs %	Depth of carburization in µm
X2	0,30	40
X3	0,52	70

CHART VI. INTENSITY OF CARBURIZATION MEASURED IN SECTIONS X2 AND X3 OF PIN 2B

In the case of pin 2C, which was otherwise identical in all respects with pin 2B, it was not possible to demonstrate the existence of any increase in carbon content in the section examined as compared with its original condition.

3 - INTERPRETATION

3.1 - Comparison of the degrees of carburization in different types of pins

The fact that a much lower degree of carburization has been observed in the type 2 pins shows that the phenomenon and the extent to which it occurs are closely bound up with the "quality" of the boron carbide used and particularly with the amount of free carbon liable to be transfered from the absorber to the sodium bond.

3.2 - Special case of pins 2B and 2C

These pins differ from pin 2A only in that they have a longer operational life (428 days instead of 304). It might have been anticipated that both the depth of carburization and the total quantity diffusing within the cladding would have been greater ; but on the contrary the carburization levels measured with the shielded micro-probe are observed to be lower than those recorded in pin 2A. Before it is attempted to explain this paradox, two important remarks must be made :

a. Where the degree of carburization is low, this phenomenon is in general very heterogeneous. This is in fact borne out by the chemical analyses made of three samples taken from portions of pin 2B located close to the sections examined with the micro-probe. The chart below gives the results of these.

Sample of pin 2B	Carbon concentration in p.p.m. (global chemical analysis)
X1	748 - 908
X2	1295 - 771
X3	832 - 837

CHART VII. CHEMICAL ANALYSIS OF SECTIONS OF PIN 2B

The special case of the value 1295 p.p.m. is particularly striking, and corresponds to a higher average degree of carburization than could be obtained by calculation with the aid of the measurements effected by shielded micro-probe in pin 2A (this method gave, e.g., 930 p.p.m. for radius 2 of sample X1).

b. The areas examined with the shielded micro-probe are very small compared with the total areas in the cladding which are liable to be carburized.

Hence one must be extremely cautious when comparing measurements effected on sections of claddings belonging to different absorbing pins, and it cannot be asserted purely on the basis of the examinations made with the electron micro-probe that pin 2A had been more seriously carburized than pin 2B and 2C.

3.3 - Calculation of the effective diffusion coefficients

The carbon distribution profiles obtained in a radial direction through the cladding were interpreted with the aid of a technological effective diffusion model which makes provision for the effects of the carbon diffusion in the austenite and of the precipitation of the type $M_{23}C_6$ carbides without distinguishing between the two. All that this type of process will reveal that will therefore be the variations in the total quantity of carbon present in the steel as determined by the distance from the inner face of the cladding.

In these circumstances, if the cladding is treated as a homogeneous plane medium, the system of equations to be solved will be as follows :

$$\begin{cases} t = 0 & C(x,0) = C_0 \\ x = 0 & C(0,t) = C_s \\ x \to \infty & C(\infty,t) = C_0 \end{cases} \qquad \frac{\partial c}{\partial t} = D_{eff.} \nabla^2 c$$

C_0 = initial carbon concentration in the steel

C_s = prescribed surface concentration

D_{eff} = effective coefficient of carbon diffusion in the steel

t = diffusion time

The solution to this problem is well known and is as follows :

$$\frac{C(x,t) - C_o}{C_s - C_o} = \frac{x}{2\sqrt{D_{eff.}\, t}}$$

In order to determine whether the carbon distribution values obtained by experimental measurement obey a law of the erfc type, it will suffice to verify the linearity of the function $\mathrm{erf}^{-1}\left(\frac{C_s - C}{C_s - C_o}\right)$ in relation to the depth x. If such is effectively the case, the inclination of the straight line in question will enable $D_{eff}.t$ to be determined, and D_{eff} to be calculated, since t is known.

The effective diffusion coefficients calculated on the basis of the above mentioned model are given in the following chart :

Pin	D_{eff} in cm^2/s	Uncertainty concerning D_{eff} in cm^2/s
1 A	$1,3.10^{-12}$	$9.10^{-13} \leqslant D_{eff} \leqslant 1,5.10^{-12}$
1 B	$8,6.10^{-3}$	$6,4.10^{-13} \leqslant D_{eff} \leqslant 1,4.10^{-12}$
2A Sample X1 radius 1	$1,4.10^{-13}$	$1,1.10^{-13} \leqslant D_{eff} \leqslant 1,9.10^{-13}$
2A Sample X1 radius 2	$3,1.10^{-13}$	$2,6.10^{-13} \leqslant D_{eff} \leqslant 3,5.10^{-13}$
2A Sample X2	$1,3.10^{-12}$	$1,1.10^{-12} \leqslant D_{eff} \leqslant 4,9.10^{-12}$
2A Sample X3	$4,7.10^{-13}$	$3,7.10^{-13} \leqslant D_{eff} \leqslant 6,3.10^{-13}$
2A Sample X4	$3,1.10^{-13}$	$2,4.10^{-13} \leqslant D_{eff} \leqslant 4,1.10^{-13}$
2B Sample X2	$5,7.10^{-14}$	$4,8.10^{-14} \leqslant D_{eff} \leqslant 7.10^{-14}$
2B Sample X3	$1,7.10^{-13}$	$1,3.10^{-13} \geqslant D_{eff} \leqslant 2,1.10^{-13}$

CHART VIII. EFFECTIVE DIFFUSION COEFFICIENTS

In the case of the type 1 pins(1A and 1B), the effective diffusion coefficients obtained are in very good agreement with the various values obtained for carbide fuel elements [5].

Results for the type 2 pins (2A and 2B) on the contrary - if we except sample X2 of pin 2A - gave us distinctly lower effective diffusion coefficients. If we are to attempt to explain these lower values, it should be recalled that use of the effective diffusion model involves an estimation of the quantity $D_{eff.}t$. Since the cladding material is necessarily characterized by a kinetic of carbon diffusion independent of the type of boron carbide used, the apparent decrease in the effective diffusion coefficient obtained by calculation would appear to be the result of over-estimation of the length of the diffusion time.

Although the values obtained for the type 2 pins would appear to reflect only mild penetration of the carbon inside the cladding (on an average in the region of 60 µm), and are therefore subject to a greater degree of uncertainty, a certain number of suppositions may nevertheless be put forward :

a. The modified boron carbide manufacturing process adopted for the type 2 pins may have produced a different type of free carbon distribution resulting in delay in the entry of the carbon into the sodium joint, which was previously held to be instantaneous. In that case the actual duration of the carbon diffusion within the steel would be far shorter than the period of reactor operation. The use of this latter value in our calculations to represent the duration of the diffusion would thus have led to relatively serious under-estimation of the effective diffusion coefficient.

b. Sample X2 of pin 2A gave us an effective diffusion coefficient roughly comparable with the values obtained for the type 1 pin, as well as for the carbide fuel elements [5], while at the same time appearing to reveal far deeper penetration of the carbon into the cladding. It may be supposed from this that the carburization of the different areas did not occur simultaneously. If that were the case sample X2 would have been carburized at the very beginning of the operational use of the pin, while the other areas observed would have been carburized far later.

These two suppositions are not mutually contradictory and may very well jointly provide the explanation.

4 - STRESSES CAUSED IN THE CLADDING

4.1 - Nature of the problem

Since the solubility limit for carbon in austenite is extremely low (50 p.p.m. at 700°C), the phenomenon of carburization is accompanied by precipitation of type $M_{23}C_6$ carbides (for the concentrations as measured in the absorbing pins). The T.T.P. (time-temperature-precipitation) diagrams for austenitic steels [7] show that from 550°C upwards the precipitation may be considered as instantaneous compared to the period of reactor operation.

The precipitation of $M_{23}C_6$ type carbides is accompanied by an increase in volume. We may thus anticipate that stresses will develop in the cladding. Following demonstration by pratical experiment of the existence of these stresses, the increase in the volume of the austenitic steel caused by the carbide precipitation will be calculated, and the distribution of the stresses through the cladding in a radial direction will be evaluated for a case considered to be representative.

4.2 - Demonstration of the presence of stresses caused by carbide precipitation

a) Experiment performed

A section of a 316 steel cladding 80 mm. in height, with inner and outer diameters 7.38 and 8.28 mm respectively was carburized in a sodium medium at 650°C for 250 hours, the carbon source being provided by an XC75 steel bar. Only the external face of the section was in contact with the sodium, and a cylindrical shield with two rectangular openings in it was placed over the section so as to create varying conditions of carburization on the circumference.

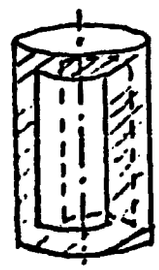

Cylindrical shield with two openings lying diametrically opposite each other, each equal in width to 1/4 of the circumference.

b) Remarks

The sample carburized was subject to the following tests :

i. Measurement

ii. Determination of the exact nature of the carburization (by chemical action and X-ray microanalysis).

The shield was found to have fulfilled its function to perfection, for the only areas found to be carburized were those in direct contact with the sodium. Fig.8 shows the profile for the carbon distribution through the cladding in a radial direction.

Measurement of the diameter (Fig.9) revealed that the irregular exposure to carburization had sufficed to cause deformation of the tubular section, the degree of ovalization being 150 µm.

c) Interpretation

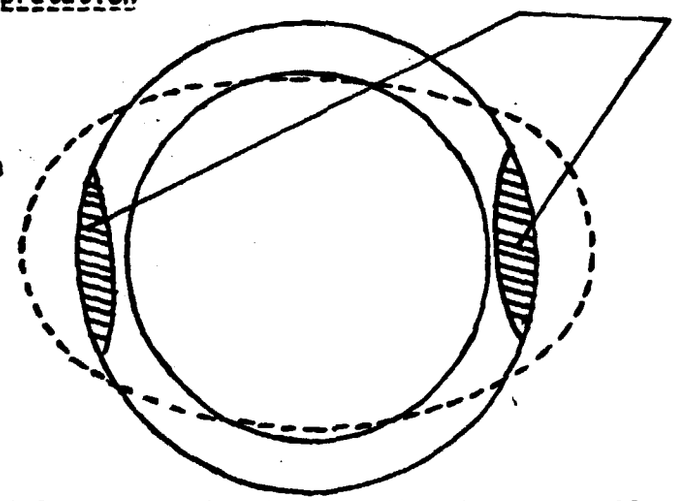

For the deformed section to have the shape actually observed the carburized area must necessarily have been under compression. We may, in fact, imagine the following mechanical equivalent :

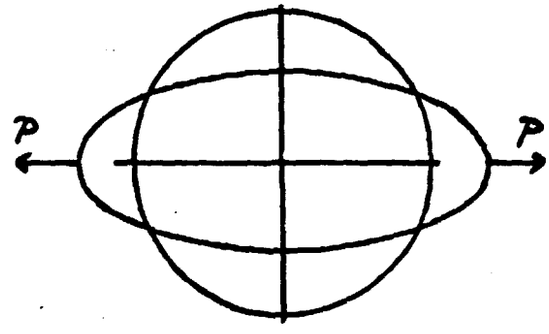

The problem is a classic one [8] and the resultant tangential stress distributions were as follows :

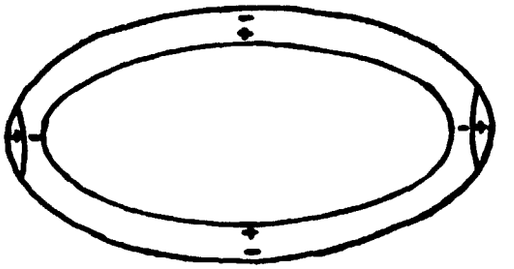

+ compression
- tension

Thus in the case of the tubular section subjected to irregular carburization, analysis of the mechanical problem involved unequivocally shows that the deformation observed can be obtained only if the carburized area is under compression. Since the only phenomenon liable to cause deformation is the precipitation of the type $M_{23}C_6$ carbides within this area, it is to be concluded that this phenomenon brings about a very substantial increase in volume.

4.3 - Calculation of the increase in the volume of the steel as a result of carbide precipitation

Since the density of the type $M_{23}C_6$ carbides is lower than that of austenite, the precipitation phenomenon is accompanied by an increase in volume. Conversely, since the Cr/Fe ratio of the carbides is higher than that of the austenite, the formation of $M_{23}C_6$ precipitates causes a loss of chronium in the matrix and hence a decrease in its volume.

Thus the results taken as a whole give us :

$$\frac{\Delta V}{V_o} = z \cdot \left(\frac{\Delta V}{V_o}\right)_1 - (1-z) \cdot \left(\frac{\Delta V}{V_o}\right)_2$$

$\frac{\Delta V}{V_o}$ = total increase in the volume of the steel

$\left(\frac{\Delta V}{V_o}\right)_1$ = increase in volume caused by carbide precipitation

$\left(\frac{\Delta V}{V_o}\right)_2$ = decrease in the volume of the austenite caused by the decrease in

its chronium content.

z = percentage of initial atoms of metal precipitating

For a 316 steel initially containing 18% of chronium, 14% of nickel and 68% of iron, we obtain, if we use the DYSON and HOLMES formula for the relation between the lattice parameter of the austenite and the chronium content [9],

$$\Delta a = 6.10^{-4} . \Delta x_{Cr} \quad \text{with a in Å and } x_{Cr} \text{ in at \%}$$

the following formula :

$$\frac{\Delta V}{V_o} = \frac{463 \times y}{100 + y} \times (0.546 - 0.193x) \quad \text{in \%}$$

x being the $\frac{Cr}{Fe + Cr}$ ratio in $M_{23}C_6$

y being the percentage of carbon precipitated

For x = 1 ($Cr_{23}C_6$ carbide), $\frac{\Delta V}{V_o} \simeq 1.65\%$ for 1% of carbon precipitated.

For x = 0.5 $\left((Cr_{0.5}Fe_{0.5})_{23}C_6 \text{ carbide} \right)$ $\frac{\Delta V}{V_o}$ = 2.1% for 1% of carbon precipitated.

Use of formula (1) presuppcses a constitent relationship between the values of y and x. In effect, for a given x ratio there exists a limit for the value of y corresponding to the total disappearance of the chronium in the metal phase. This figure is obtained by

$$y_{lim} = \frac{1.014}{x - 1.014 \times 10^{-2}}$$

Fig.10 shows the extent of the admissible field for x and y.

4.4 - Calculation of the stresses produced in the cladding

As a practical example we will take the case of pin 1A, the pin in which the highest degree of carburization was observed. The distribution profile found to exist after 368 days in the reactor did not develop instantaneously, and its progressive development with the passing of time must be determined by correct calculation.

If we use the effective diffusion model mentioned earlier on, the carbon concentration at time t in an internal fibre of the cladding located at a distance x from the inner face of the latter will be expressed as follows :

$$c(x,t) = c_0 + (c_s - c_0)\ \mathrm{erfc}\left(\frac{x}{2\sqrt{Dt}}\right)$$

where $D = 1.3 \times 10^{-12}$ cm²/s

Most of the carbon is assumed to have precipitated, though this is probably a very pessimistic view. It is further estimated that a 1% carbon precipitation causes a local swelling of 1.8% (§ 5.3). Hence the effect of the carburization on the cladding will be to produce a local swelling determined by the following equation :

$$\frac{\Delta V}{V}(x,t) = 0.018\ \left(C_0 + (C_s - C_0)\ \mathrm{erfc}\left(\frac{x}{2\sqrt{Dt}}\right)\right)$$

The mechanical calculation of the stresses in the cladding was carried out with the aid of the TUREN Code [10] on the basis of the mechanical properties of an irradiated 316 steel capable of deformation by irradiation and thermal creep. To avoid introducing discontinuities into the calculations it was assumed that the internal fibre of the cladding had the same swelling rate as the steel in the area lying 10 µm from the inner face of the cladding. With the aid of this expedient it was possible to introduce kinetics into the study of the deformations on the inner face of the cladding ; naturally these kinetics had a physical significance, since at the temperature involved (500°C) the precipitation phenomenon was far from being instantaneous.

The results of the above calculations are shown in Figs.11, 12, 13 and 14.

Fig.11 shows the gradual develoment of the deformations necessarily caused by the precipitation phenomenon, as calculated with the aid of formula (2).

Fig.12 shows the development of the distribution of the tangential stresses in the cladding as irradiation proceeds. To put it very roughly, the carburized area is subjected to compression stresses and the non-carburized area to tensile stresses (moment in the section : nil). The level of the compression stresses, which can be extremely high, is the result of the race between :

a. The deformation caused by the carbide precipitation, and

b. The relaxing of the stresses through irradiation creep.

The race between the two affords a satisfactory explanation for the development of the stresses on the inner face. Thus from the 2nd to the 10th day the very rapid rate of deformation causes the level of the stresses to rise. Subsequently this rate decreases and a decrease in the level of the stresses is to be observed as a result of the relaxation caused by irradiation creep.

Fig.13 shows the development of the plastic deformation of the inner face of the cladding with the passing of time. The temperature is too low for any significant deformation through thermal creep. The two processes of plastic deformation are thus to be explained by :

a. The irradiation creep, which accounts for practically the whole of the deformation and for all deformation occuring after the 10th day ;

b. The instantaneous plastic deformation which occurs during the first ten days, i.e. so long as the level of the stresses at the inner face of the cladding is very high.

The total amount of plastic deformation of the inner face of the cladding is considerable, since it exceeds 1%.

Fig.14 shows the development of the macroscopic plastic deformation of the cladding, which, though significant, is still only mild after 368 days of irradiation.

5 - INFLUENCE OF CARBURIZATION ON THE MECHANICAL PROPERTIES OF THE CLADDING.

Before we go on to look at the possible effects of carburization on the mechanical properties of the cladding, it should be recalled that the latter is at the same time subjected to the cumulative and sometimes conflicting effects of integrated dose and temperature. These parameters vary from one point to the next from one end to the other of the control rod pins. Further, in the absorbing element, whose essential attribute is mobility (in the upper part of the core) the dose-temperature parameter frequently varies according to control requirements between limits as to duration and depth which are difficult to determine with accuracy.

Under such conditions it is not easy to demonstrate the influence of carburization on the mechanical properties of the cladding material. However, a certain number of tensile tests were carried out on circular samples taken from pins 1B, 2A and 2B.

5.1 - Tensile tests made on sample rings

The samples used for these tests were rings measuring 5 mm in a vertical direction, cut from the cladding in a direction perpendicular to its axis. They were chosen for the following reasons :

a. Extreme ease with which they could be obtained from a tubular component by an ordinary cutting stroke after elimination of the boron carbide.

b. Convenient way in which the rings could be secured in line on the tensile test machine with semi-circular grips fitting the inner diameter of the tube.

c. Radial stress similar to that obtaining under extreme operating conditions (internal thrust exerted by the absorber in the event that the gap should be filled).

d. Low gradient for the irradiation parameters on the 5 mm. vertical dimension.

The testing temperature of 400°C was chosen to ensure that in all cases the tests would be performed at far less than the irradiation temperature, in order to avoid any risk of restoration while they were in progress.

The stresses developed slowly, at about 1%/min. Chart IX gives the complete results obtained for the various pins.

Height from lower part of pin (in mm)	R Tensile strength in daN/mm²	Eo Yield point in daN/mm²	A % distributed	A % total
Pin 1B				
60	73,1	61,2	0,6	0,6
66	71,8	64,5	0,6	0,6
Pin 2A				
25	94,2	85,4	1,6	2,6
38	94,6	82,9	2,3	3,2
66	91,2	78,8	2,4	5,4
101	83,8	74,5	2,5	5,3
107	86,4	75,5	2,3	5,3
139	93,3	78,7	2	5
920	66,2	51	5,9	10,8
Pin 2B				
15	94,1	75,1	1,8	2,4
21	92,1	74,3	1,8	2,6
27	89,6	74	2,2	4,2
33	86,6	68,2	2,5	3,8
39	86,3	68,9	2,3	3,6

CHART IX. MECHANICAL PROPERTIES

5.2 - Interpretation

The variations recorded in the yield point according to the level at which the sample had been taken (Fig.15) showed that a distinct decrease occurred as the height above level 0 increased ; this was to be anticipated, since the dose, and hence the degree of hardening, grow less severe as one travels up the pin, whereas the temperature is constant or even slightly on the increase.

The comparison between the results obtained for the various pins may, on the contrary, cause some surprise, since, with due allowance for the height at which they were located, the most severely irradiated samples (pins 1B and 2B) appeared to be less "hardened" than those taken from pin 2A. In reality, the fact that the temperature was maintained above 500°C (304 days of restoration for 2A as against 368 and 428 respectively for pin 1B and 2B) cancealed the effect of the dose.

It is further to be noted that the one test made at a level not subjected to flux, i.e. at the top of the pin (2A), produced results very close to those obtained for the same material when not irradiated.

The ductility measurements (Fig.16) revealed relatively serious embrittlement in the case of pin 1B (A% distributed : 0.6%). It was in fact in this precise instance that the highest degree of carburization was observed (§4), and it would look as though at this level ($C_s \simeq 1.5\%$) the result is a decrease in the ductility of the metal.

In the case of the other pins examined, where the carburization was distinctly less severe (in both intensity and depth), the ductility values obtained under testing conditions remained perfectly acceptable for irradiated steel of the type, since they scarcely fell below 2%.

As in the case of the yield point, the values obtained at levels not subjected to flux were roughly equal to those recorded for the same metal when not irradiated.

CONCLUSION

With the aid of X-ray microanalysis and micro-hardness techniques it was possible to study the phenomenon of carburization in the cladding of the absorbing elements in fast breeder reactors. A comparison of the results obtained

for different types of pins showed that the intensity and depth of the carburization were closely connected with the quantity of free carbon present in the boron carbide.

The diffusion of the carbon in a radial direction through the cladding is accompanied by the phenomenon of precipitation of type $M_{23}C_6$ carbides. These produce stresses which may reach severe levels at the initial stage of the irradiation.

The mechanical properties of the cladding steel are not seriously affected by the carburization phenomenon. The only case in which a decrease in ductility was found to occur was that of pin 1B, which showed the highest degree of carburization of all those examined.

REFERENCES

[1] K. NATESAN, T.F. KASSNER and CHE-YU
Reactor Technology, Vol.15, N° 4 (Winter 1972-1973)

[2] R.B. SNYDER, K. NATESAN, T.F. KASSNER
Journal of Nuclear Materials, 50 (3), pp.259-274, April 1974

[3] F. COPPOLA, F. MAURICE and J. RUSTE
8th International Congress on X-Ray Optics and Microanalysis, Boston, August 1977.

[4] M. CHAMPIGNY, D. GAUVAIN, L. MENY and J. RUSTE
8th International Congress on X-Ray Optics and Microanalysis, Boston, August 1977

[5] R. CYTERMANN, M. PERROT, J. ROUAULT
International Conference of the BRITISH NUCLEAR ENERGY SOCIETY :
"Post-Irradiation Examination"
Grange-over Sands (England), May 1980

[6] R. CYTERMANN, M.PERROT
A.N.R.T. meeting : "Microsonde et Microscopie Electronique à Balayage"
Karlsruhe, 23 and 24 June 1981

[7] B. WEISS, R. STICKLER
Metallurgical Transactions, Vol.3, April 1972, 851

[8] S. TIMOSHENKO
Résistance des matériaux (Dunod, 1968).

[9] D.J. DYSON, B. HOLMES
Journal of the Iron and Steel Institute, p.469, May 1970

[10] Y. GUERIN
I.W.G.F.R. - 31 -P28 (Fontenay-aux -Roses, 1979).

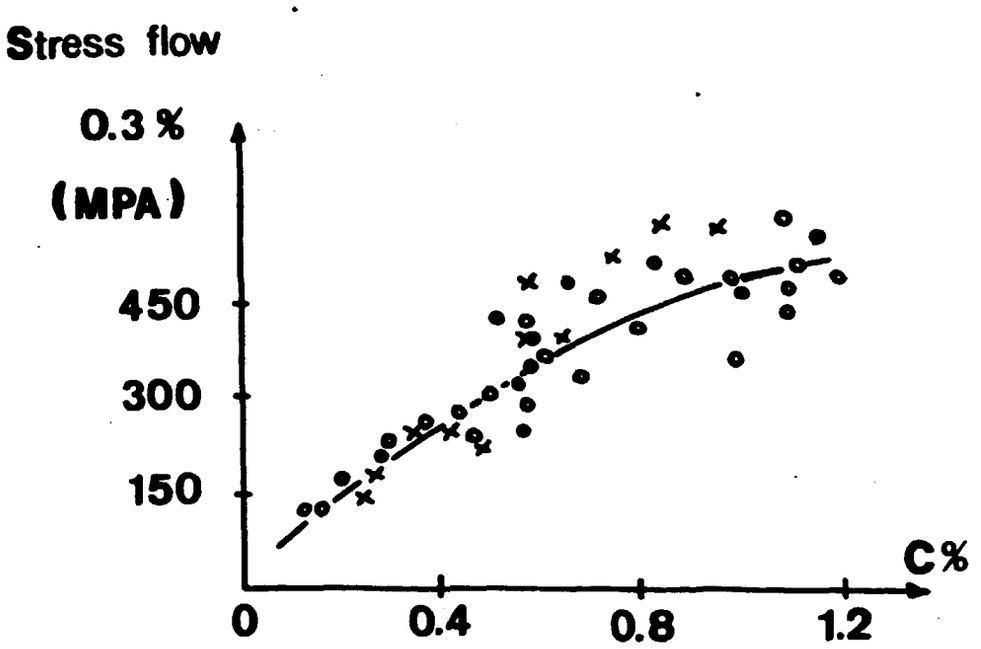

Fig.a - Stainless steel 316 stress flow versus carbon content

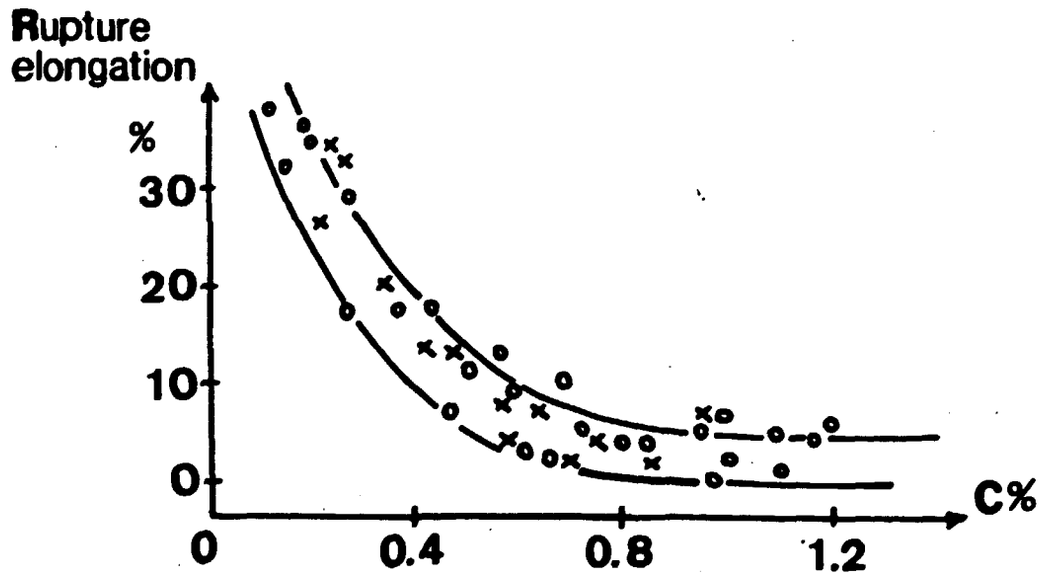

Fig.b- Stainless steel 316 rupture elongation between 500 and 800°C versus carbon content

from [1]

Figure 1

Stainless steel 316 mechanical properties evolution versus carbon content

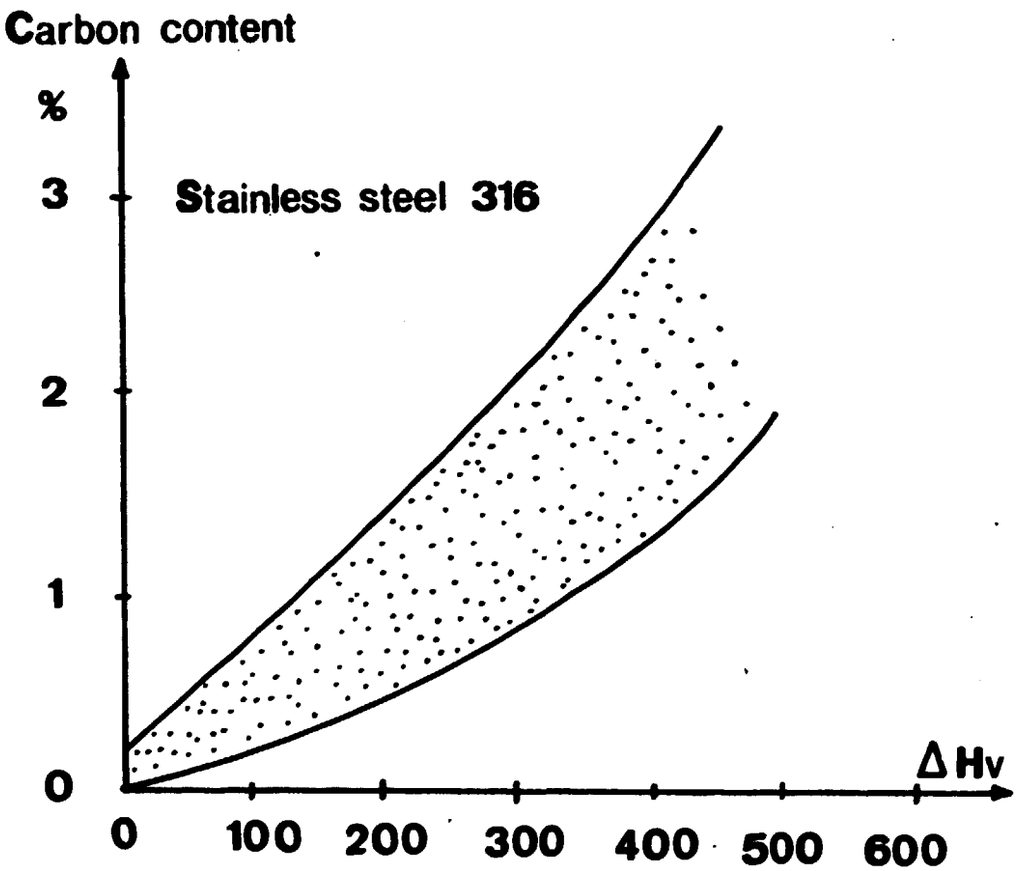

Figure 2

Hardness increase versus carbon content (from [6])

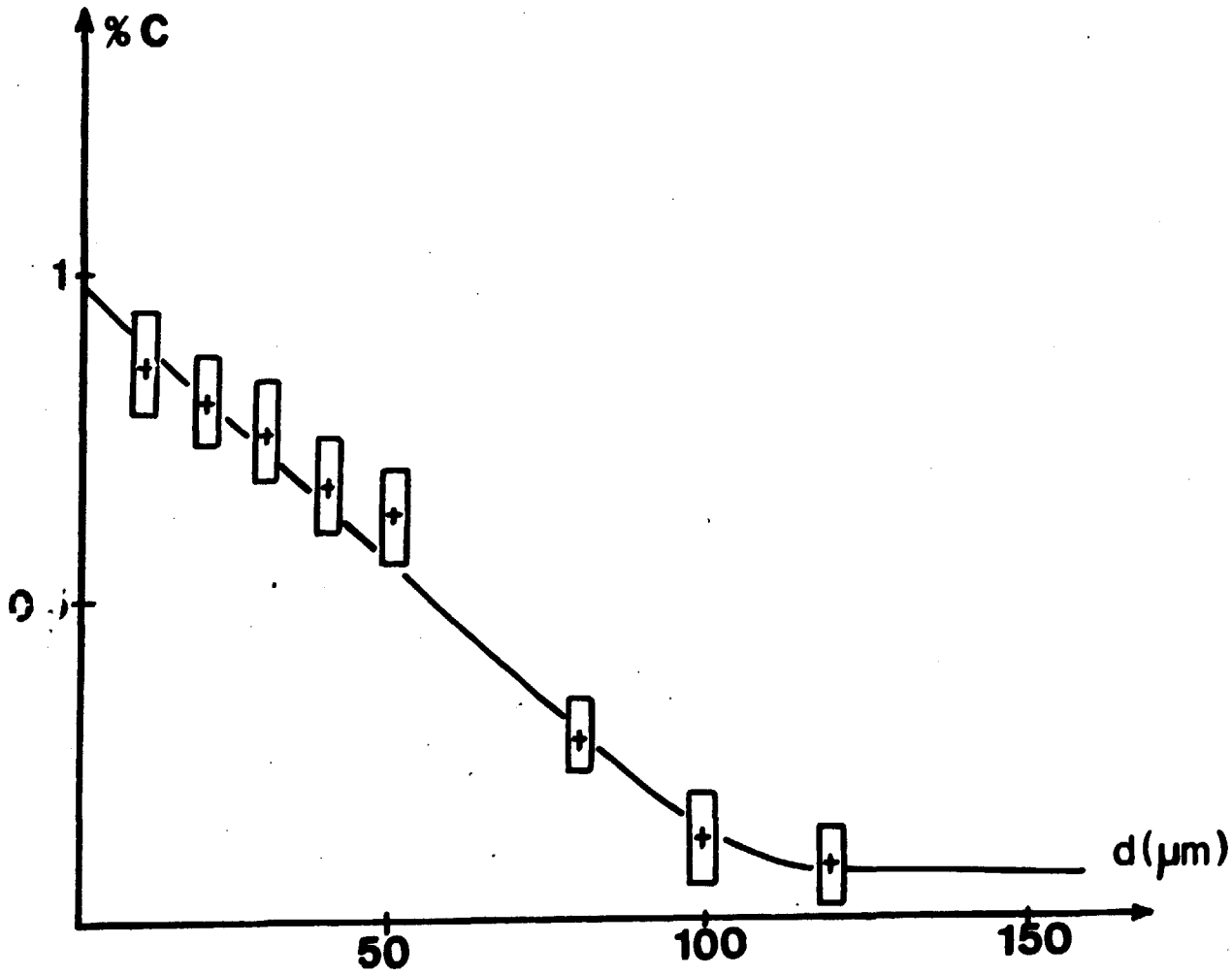

Figure 3

Carbon distribution – Absorbant pin 1A

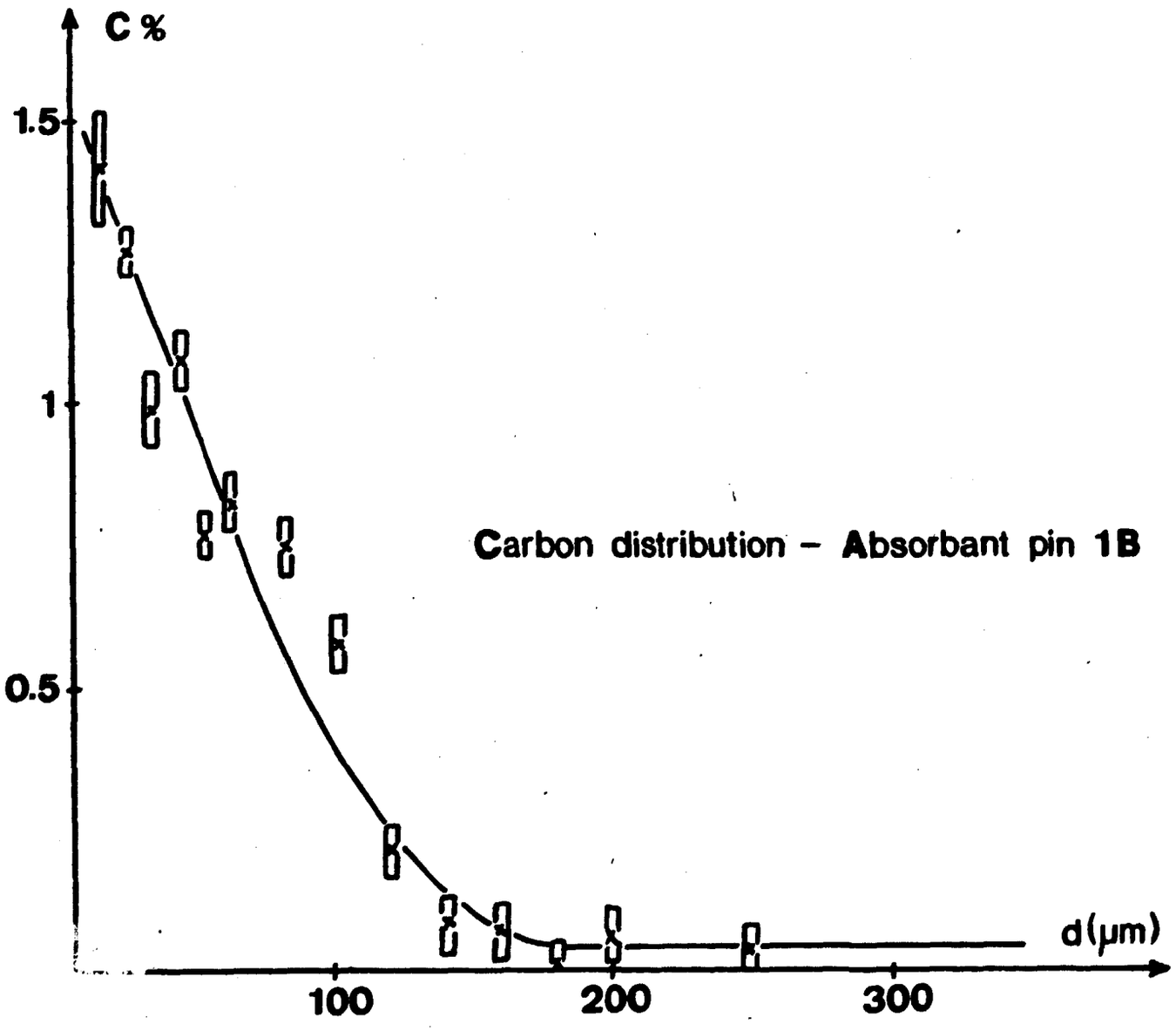
C %
1.5
1
0.5
Carbon distribution – Absorbant pin 1B
d(µm)
100
200
300

Figure 4

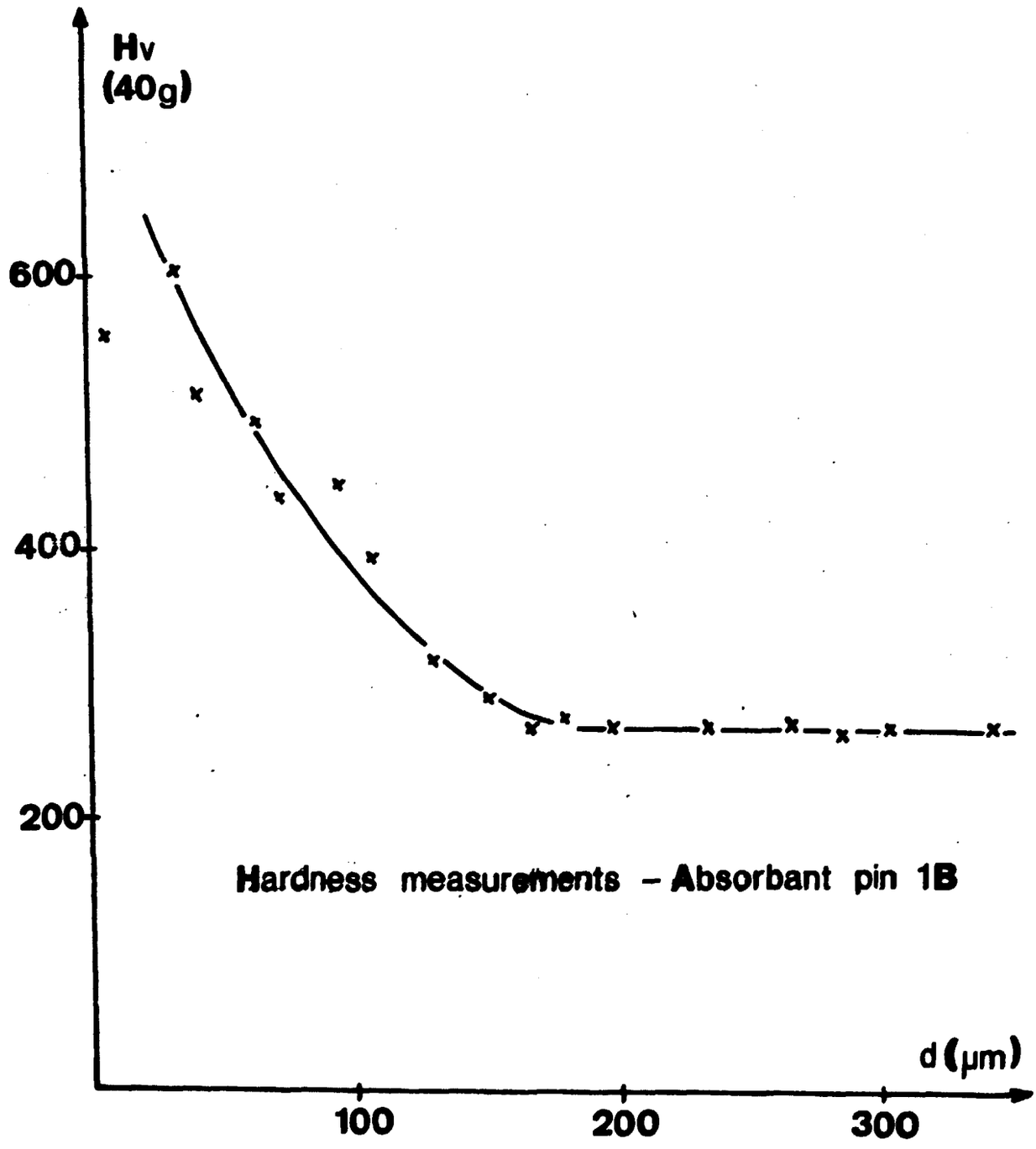

Hardness measurements – Absorbant pin 1B

Figure 5

Concentration measurements at 20 µm
from the inner face of the cladding

123...

Carbon distribution - Absorbant pin 2A

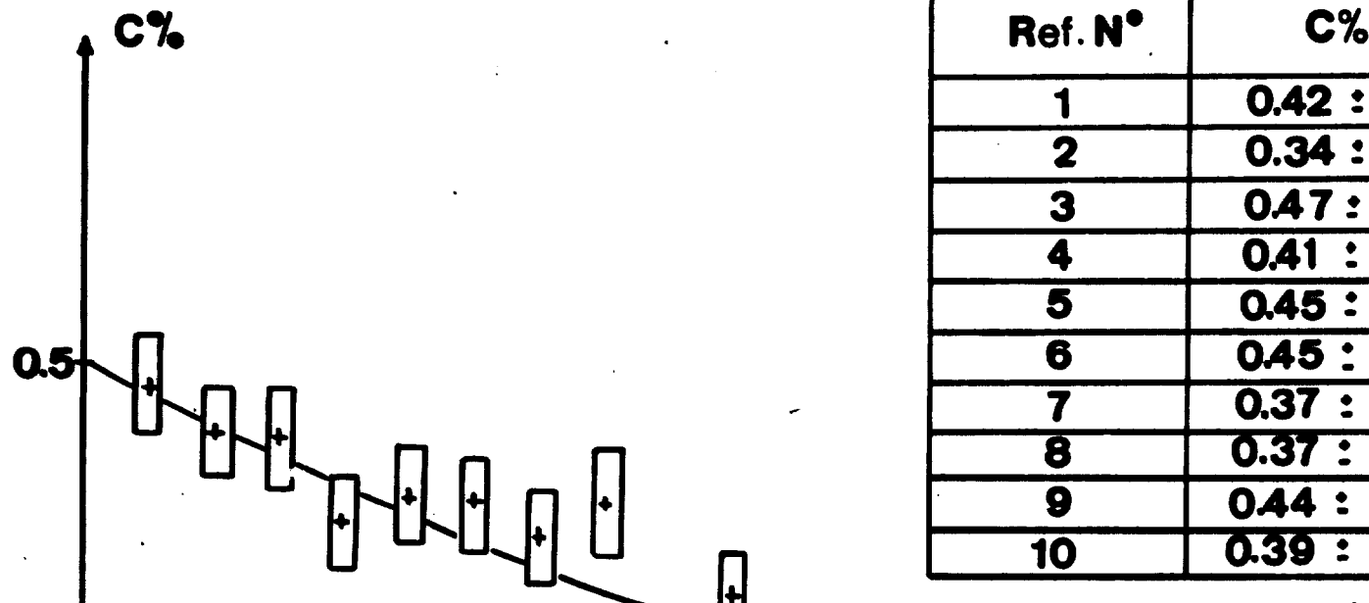

Ref. N°	C%
1	0.42 : 0.04
2	0.34 : 0.04
3	0.47 : 0.03
4	0.41 : 0.05
5	0.45 : 0.02
6	0.45 : 0.09
7	0.37 : 0.07
8	0.37 : 0.07
9	0.44 : 0.08
10	0.39 : 0.07

Figure 6

Carbon distribution - Absorbant pin 2B

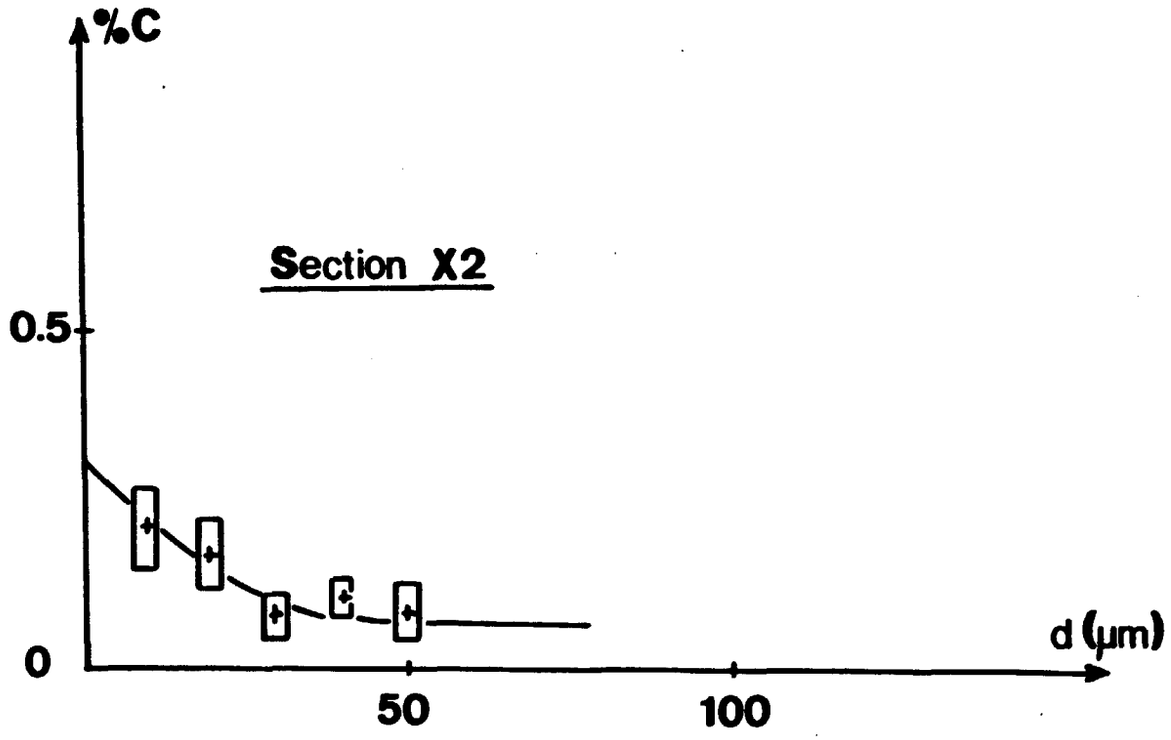

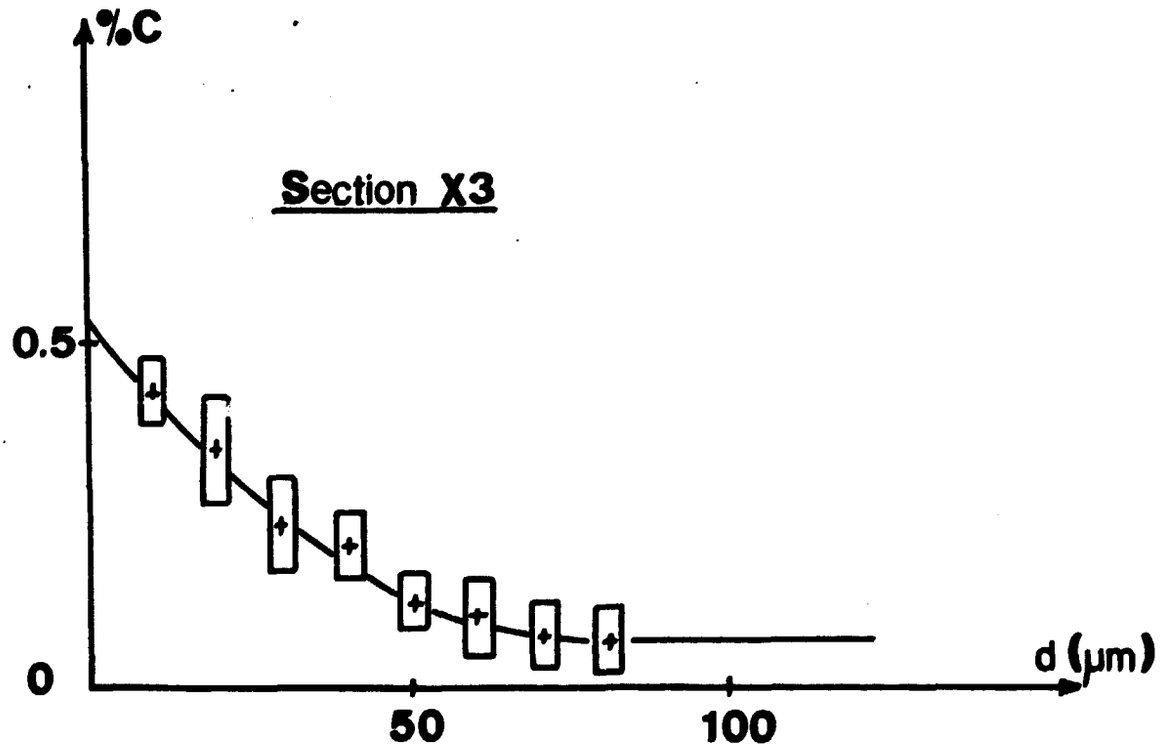

Figure 7

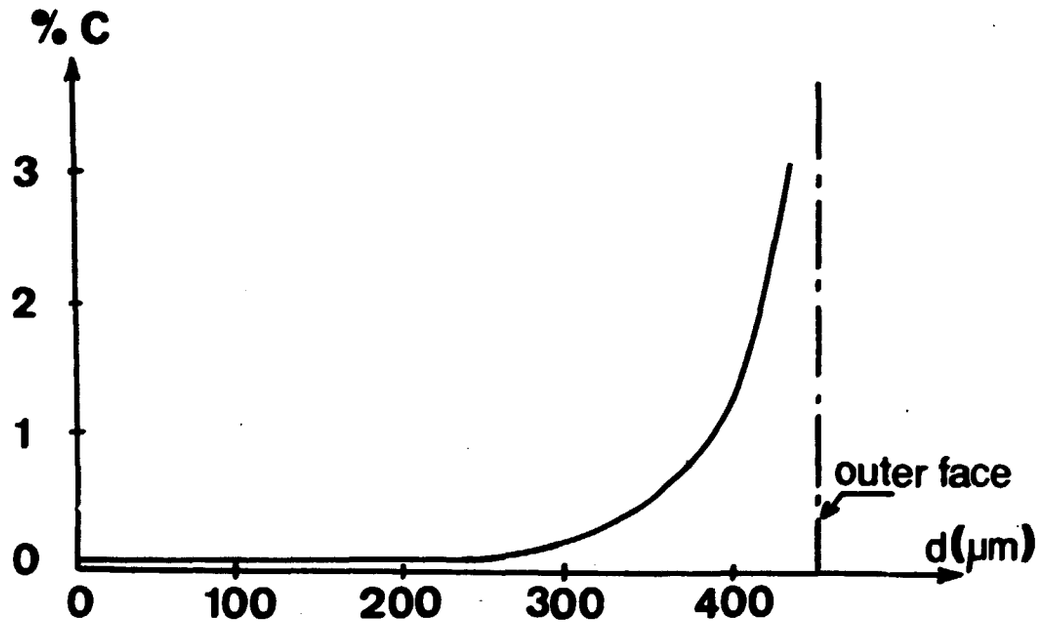

Carbon distribution – Simulation experience

Figure 8

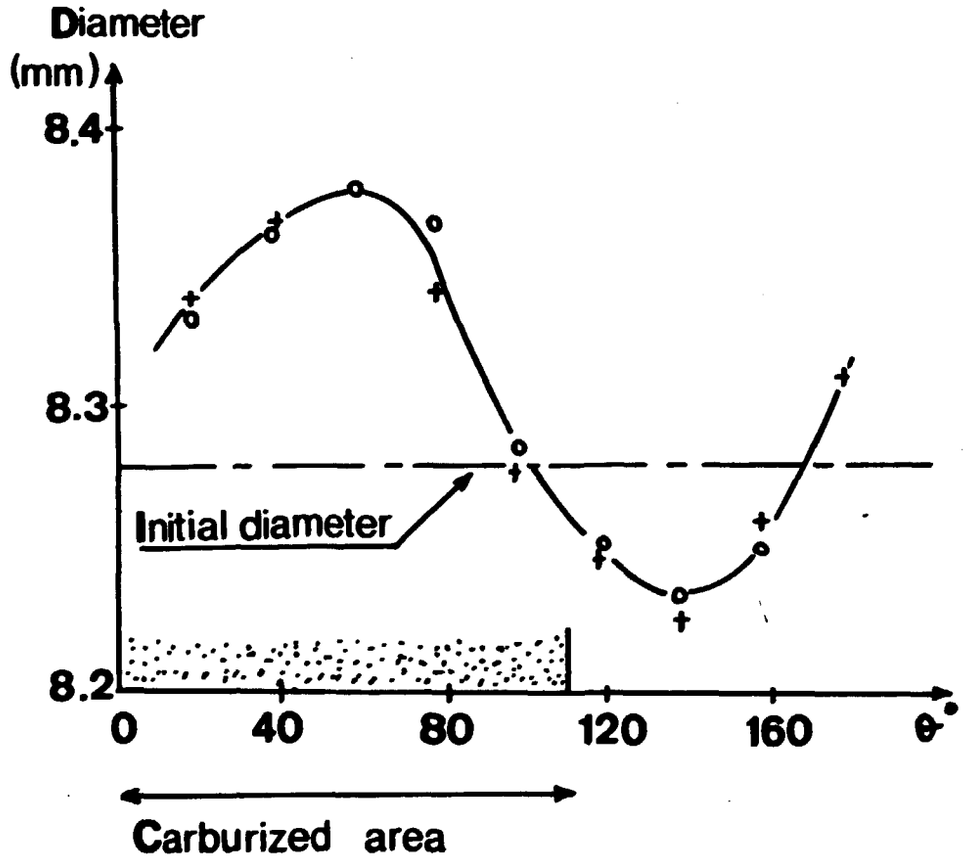

Metrology_

Figure 9

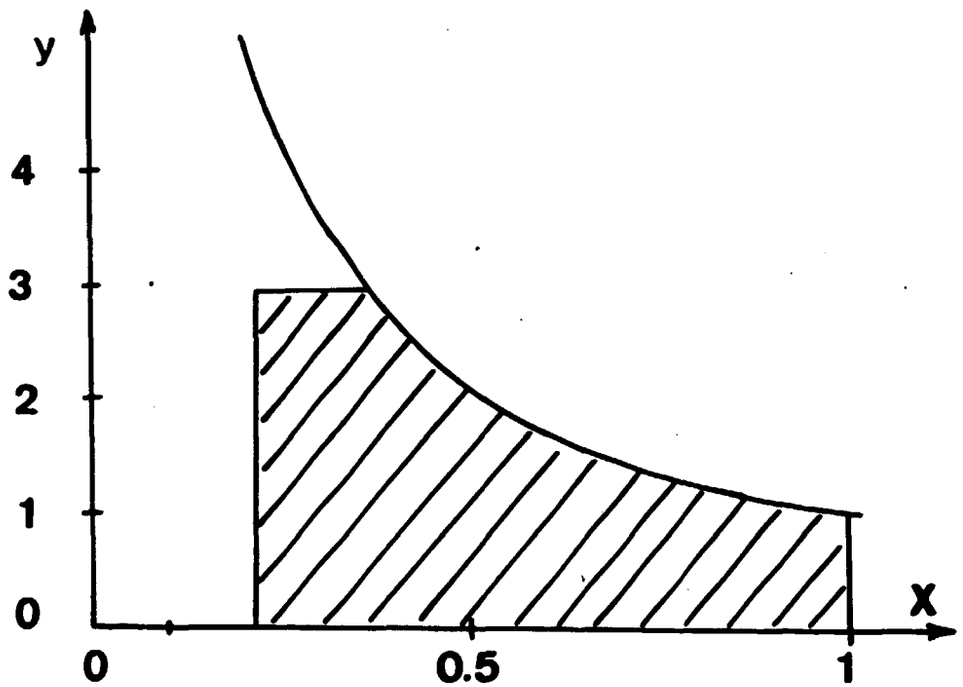

Admissible field for X and y

Figure 10

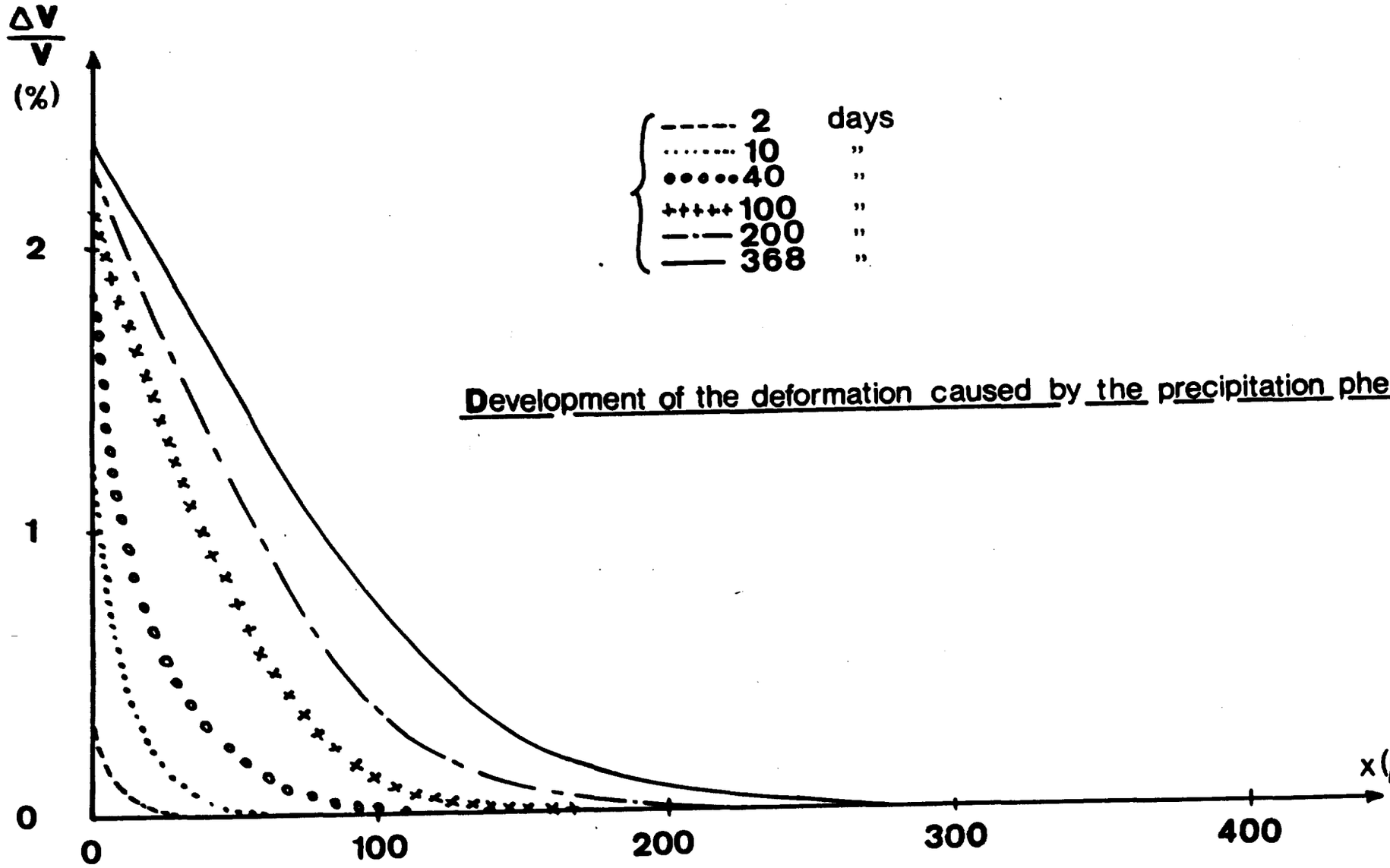

Development of the deformation caused by the precipitation phenomena

Figure 11

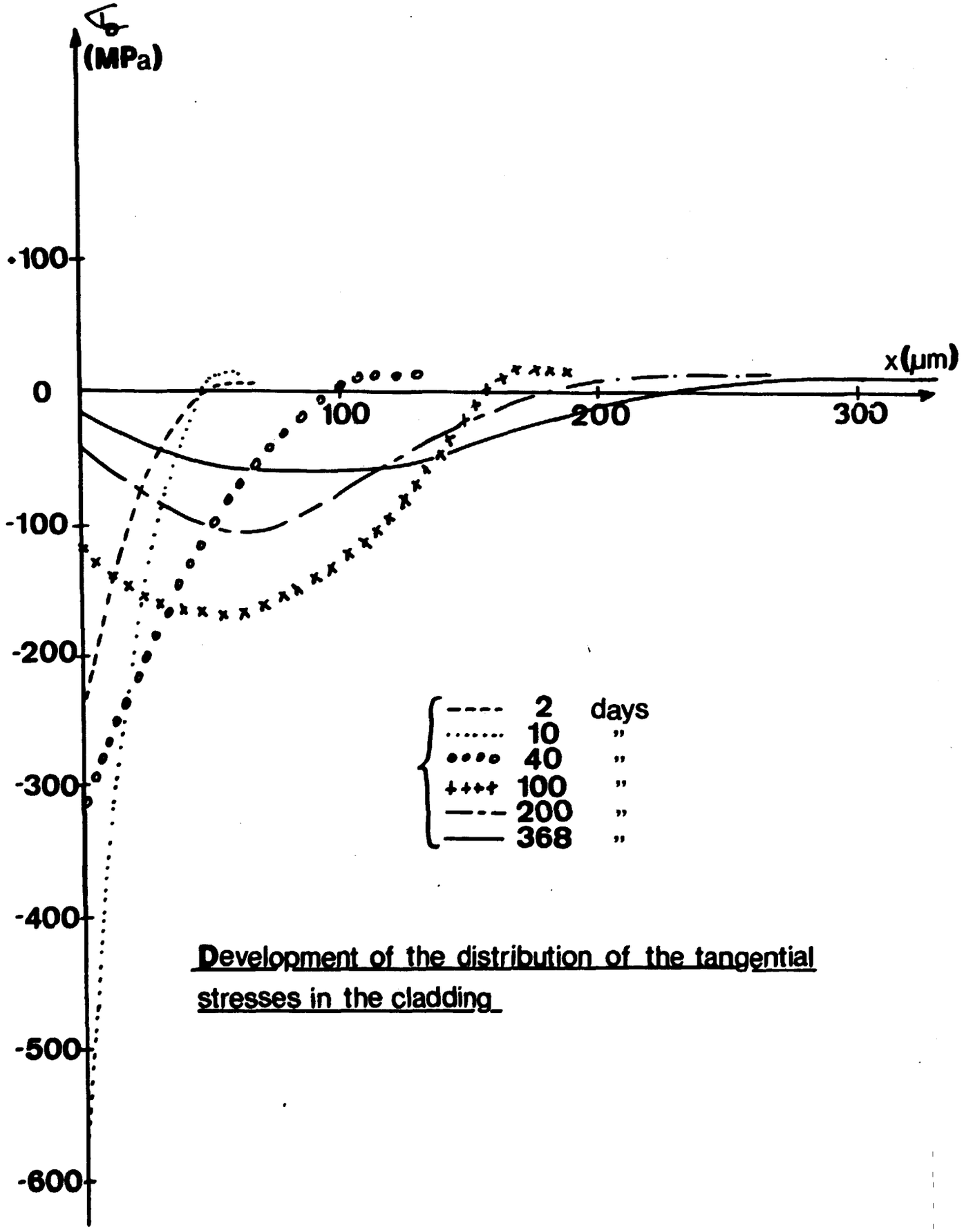

Development of the distribution of the tangential stresses in the cladding

Figure 12

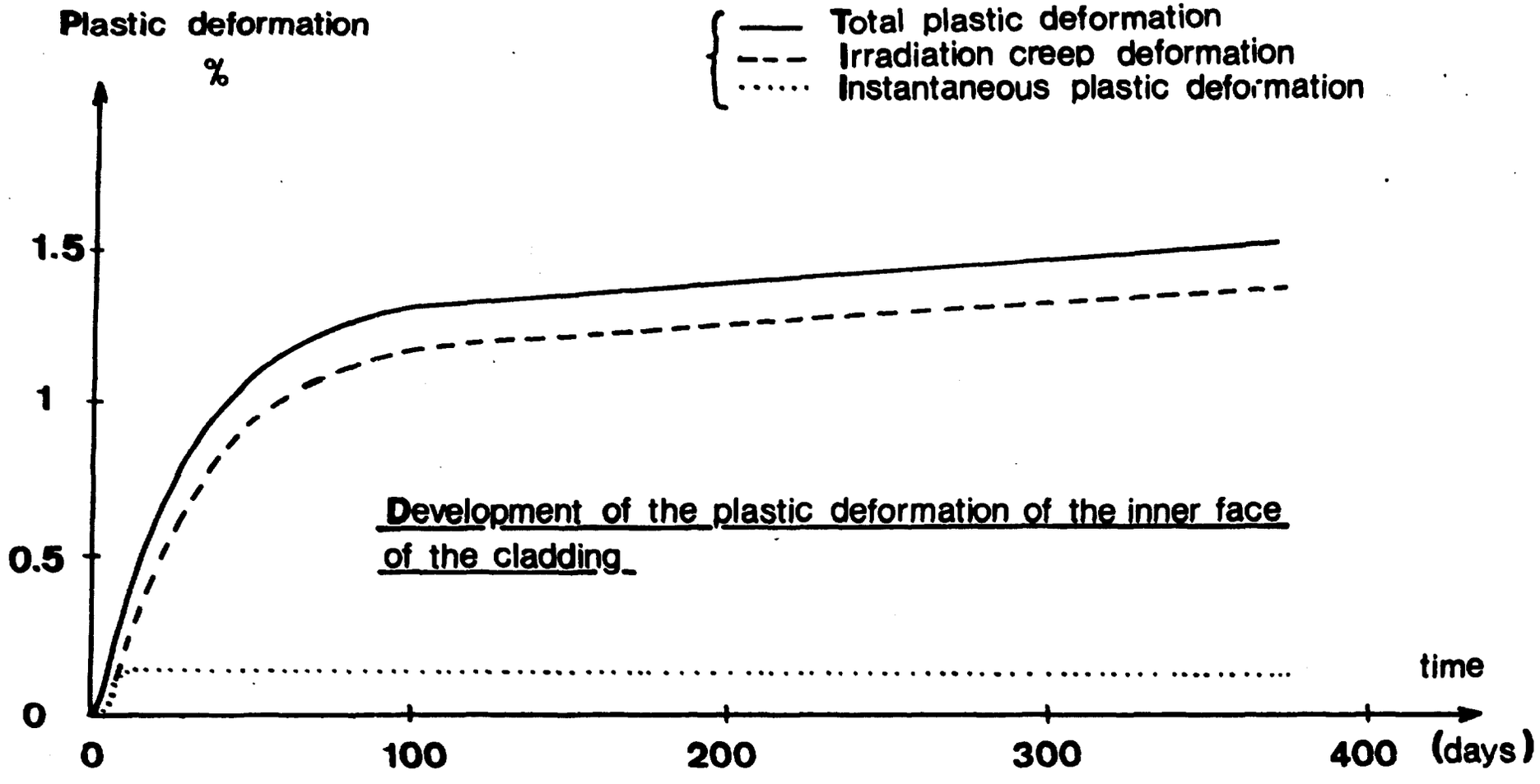
Plastic deformation
%
Total plastic deformation
Irradiation creep deformation
Instantaneous plastic deformation
1.5
1
0.5
0
Development of the plastic deformation of the inner face of the cladding
time
0
100
200
300
400
(days)

Figure 13

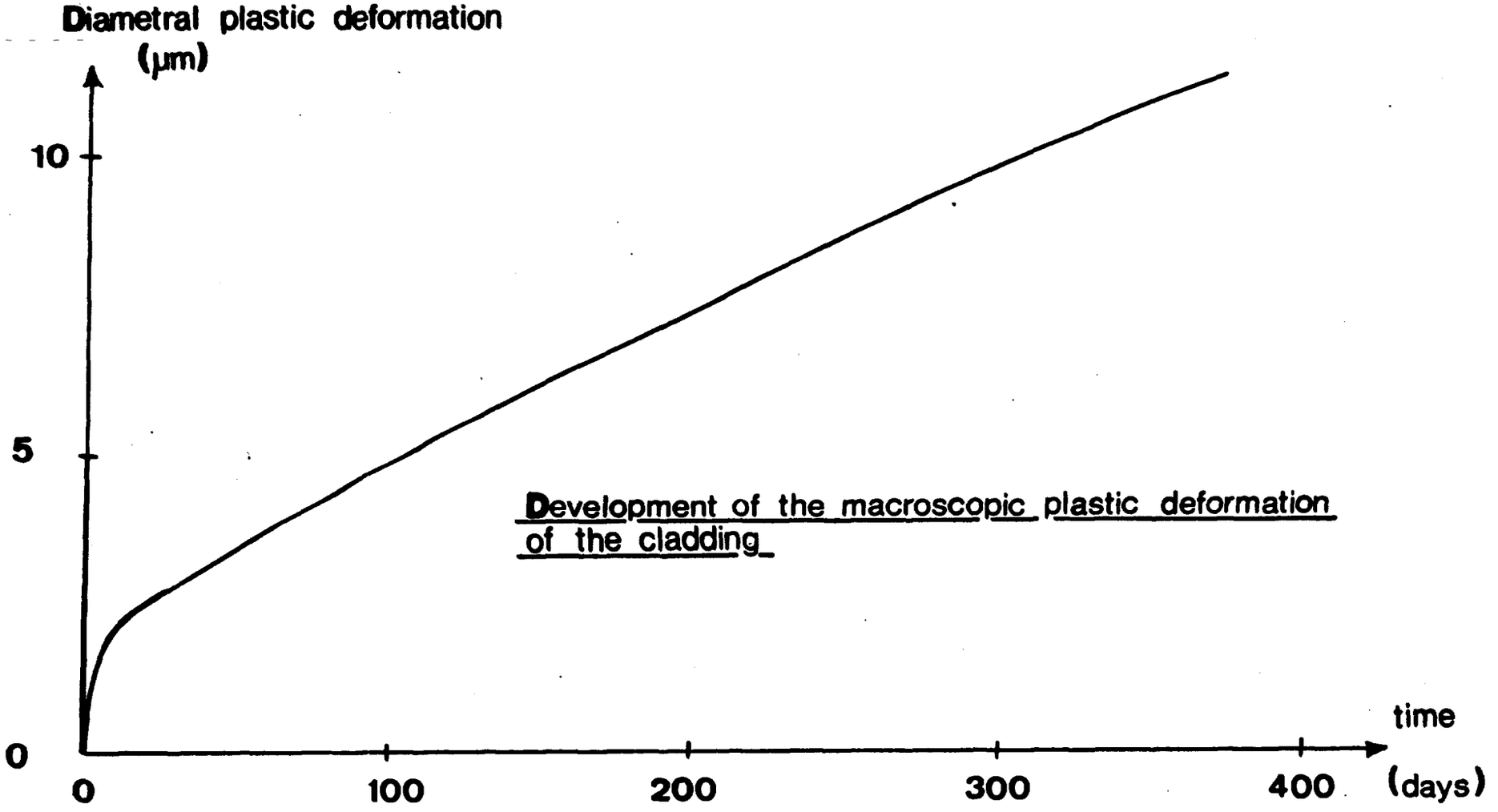

Development of the macroscopic plastic deformation of the cladding

Figure 14

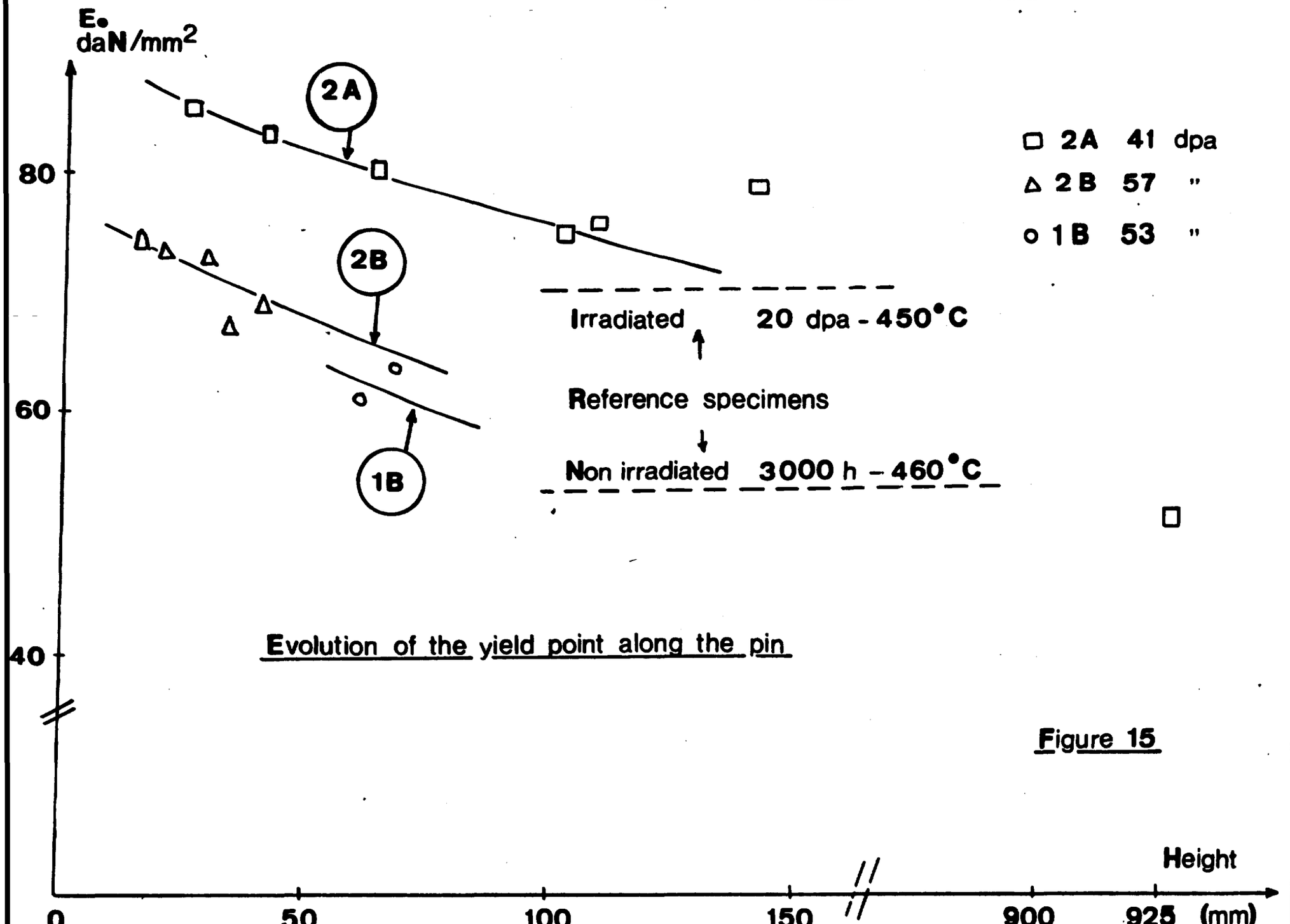

Evolution of the yield point along the pin

Figure 15

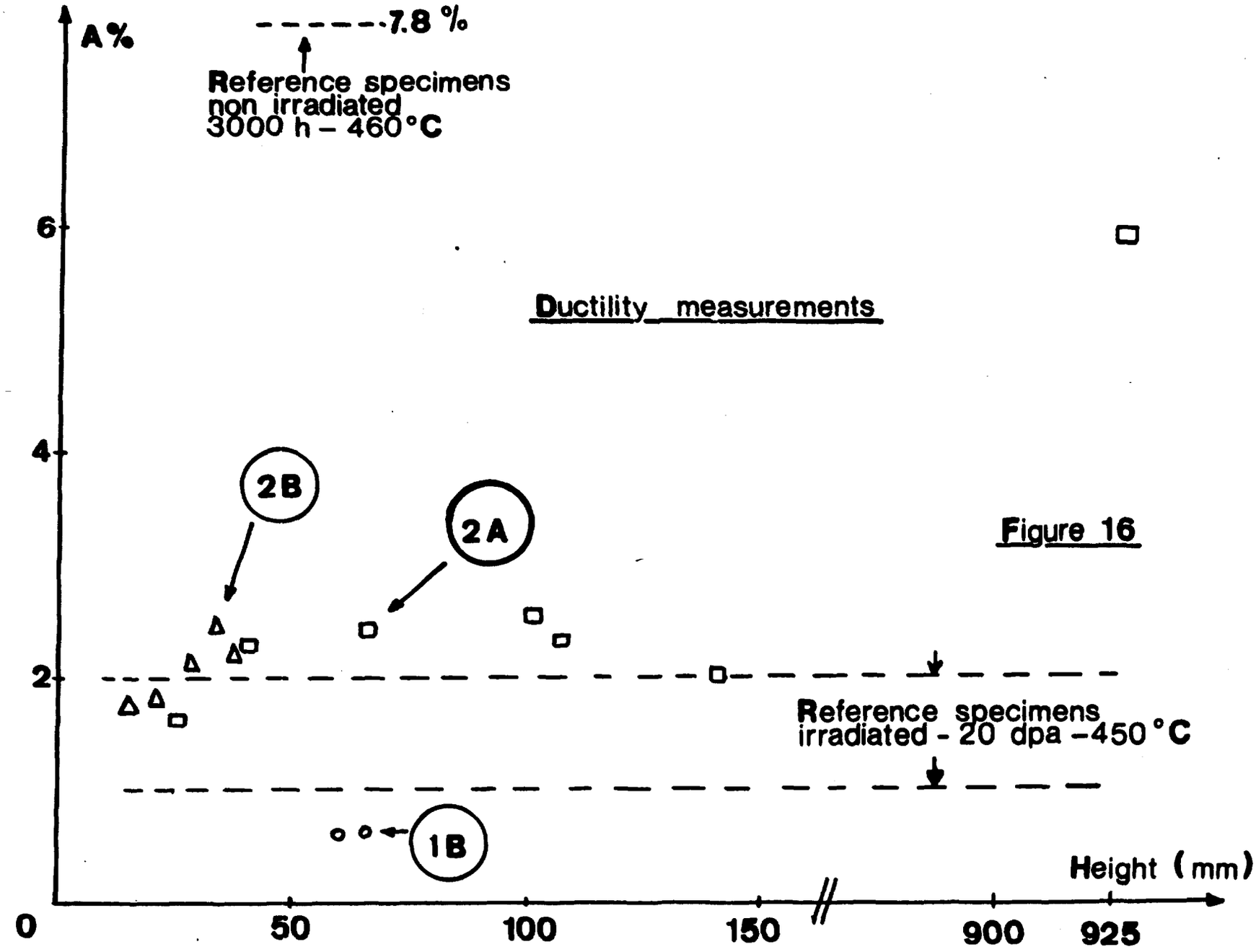
A%
7.8 %
Reference specimens
non irradiated
3000 h – 460°C
6
4
2
0
Ductility measurements
2B
2A
1B
Reference specimens
irradiated - 20 dpa –450 °C
Height (mm)
50
100
150
900
925

Figure 16